11 Application of the basic design of the dual thin film probe for total temperature measurements behind a cascade in CT2

11.1 Introduction

The operation of the dual thin film probe is tested for several repeatable tests behind a cascade in the VKI CT2 Isentropic Light Piston facility (paragraph 1.5). The gas temperature is also evaluated by means of a thermocouple placed upstream of the cascade. Not only the basic design of the probe is described, but also the limitations of the Plexiglas and Ertalon support are discussed. The agreement between the results of the probe and the ones of the thermocouple is satisfactory.

11.2 Test Conditions and probe design

The measurement principle of the dual thin film probe is described in paragraph 10.2 and the gas temperature, T_{GAS}, determination is possible through Eq. (45). During the test, the two wall temperatures (T_{W1}, T_{W2}) are directly measured and the corresponding wall heat fluxes (Q_{W1}, Q_{W2}) are calculated by solving the one dimensional heat conduction equation inside the gauges surface for every time step (paragraphs 10.3 and 10.4).

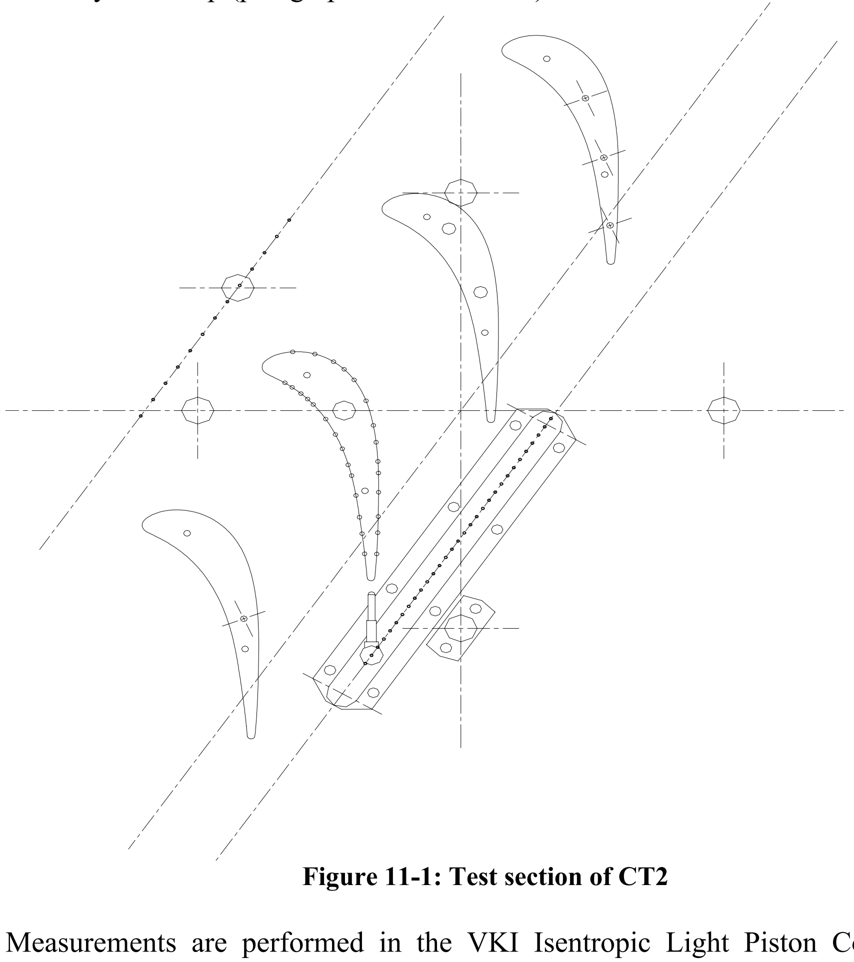

Figure 11-1: Test section of CT2

Measurements are performed in the VKI Isentropic Light Piston Compression Tube facility CT2 (Consigny et al., 1979). The test section is instrumented with a four-bladed linear cascade, shown in Figure 11-1. The dual thin film probe is placed downstream on a pneumatic traversing mechanism. The upstream total temperature is measured by a thermocouple. Measurements are taken at high Reynolds number (*900,000*) and at exit isentropic Mach number equal to *1.1*. The Reynolds number is based on the actual chord (*120.5mm*) and on the isentropic exit conditions whose values are controlled by the upstream total pressure and temperature. The exit isentropic Mach number is computed by using the upstream total pressure and the measured static exit pressure. The upstream total temperature is set equal to *390K* (target value) and the upstream Mach number is measured equal to *0.4*.

The dual thin film probe is designed to measure a two dimensional flow field (Figure 11-2). The symmetry plane, where the length of the thin film sensors is located, matches with the equivalent one of the trailing edge of the blades used in the test section in the CT2 facility. The signal is carried till the bottom part of the cylindrical heads by golden thin films, from where it is transferred to the Wheatstone bridge by cables. The optimization in space of the probe requires *4.2 mm* distance between the two axes of symmetry of the heads, leaving only *0.5 mm* support material between the two ceramic heads (Figure 11-3). Note that a design of minimum width of the probe is of primary importance, because the two heads should feel the same flow in order Eq. (45) to be applicable for gas temperature calculations.

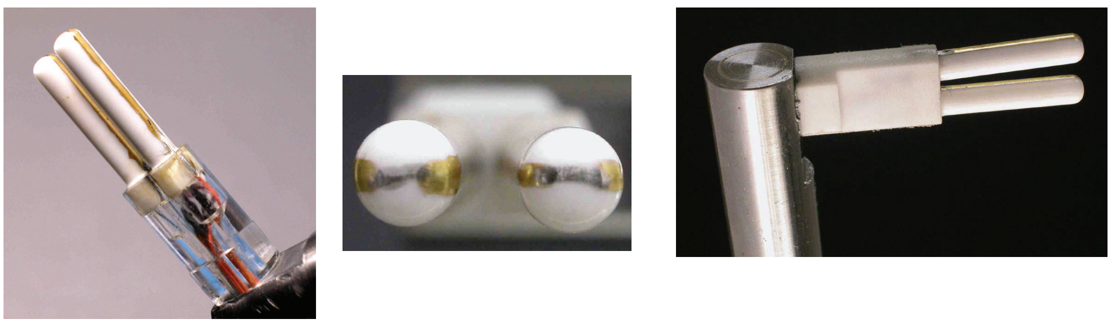

Figure 11-2: The dual thin film probe made of Plexiglas and Ertalon support

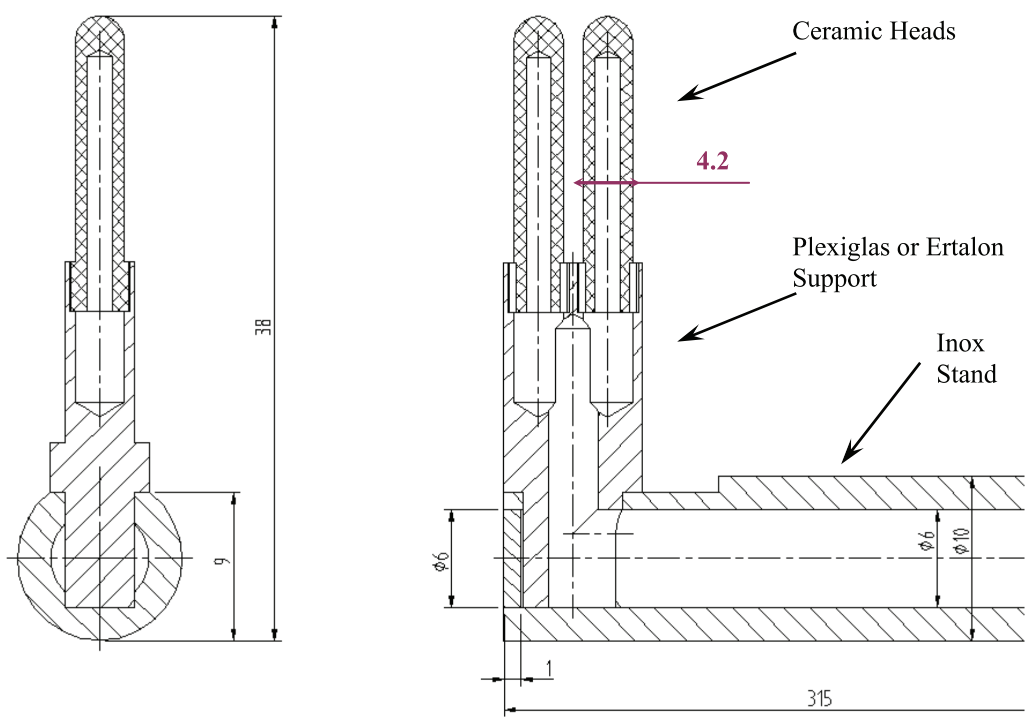

Figure 11-3: Design of the dual thin film probe used in CT2 (all dimensions in mm)

The interior diameter of the ceramic head is adapted to contain the resistance of the heating element. Due to manufacturing constrains the exterior diameter is *3mm*. However, the lowest part of the ceramic is enlarged in order to create a suitable gap (*0.25mm* at each side) where the two signal cables (shown in blue for one gauge and red for the second gauge in Figure 11-4) are connected to the golden thin films. The heating element is powered by a *12V* battery supply; because of the high current passing through the connections of the element with the battery, there is the need of splitting this current into two cables for each connection (4 cables in total with orange color in Figure 11-4). The dimensions of the cables are also given in Table 11-1.

Not only the space limitations of the probe combined with the fact that one of the two heads is strongly heated, but also the above electrical connections require a suitable material selection for the support of the two heads. It has to be both electrical and thermal insulating such as advanced plastics. (Note that ceramic fulfills the above limitations, however it cannot be machined in such small width dimensions.) The selected plastics are presented in Table 11-2 together with their most important properties for our case. The maximum temperature of the material limits the maximum heating temperature of the probe and the dilatation coefficient demonstrates the dilatation levels of the selected plastics in comparison to ceramic heads. Note that Ertalon and mostly Plexiglas are widely used in turbomachinery applications, mainly because they are easily machineable and cheap. This is the reason why two supports are made from these two materials for the basic design of the dual thin film probe. However, the final design of the probe described in chapter 12 is based on supports made of Vespel, because of the higher maximum temperature of use.

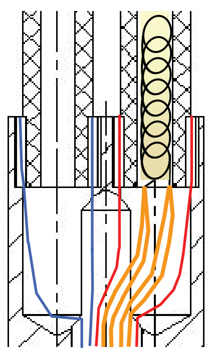

Figure 11-4: Connections

No of wires	Area	Colour
4	*0.1089 mm²* (d = 0.33 mm)	Red & blue
4	*0.25 mm²* (d = 0.5 mm)	Orange

Table 11-1: Cable dimensions

Material	Max. Temperature of use (K)	Temperature of softening point (K)	Dilatation coefficient (10^{-6} m/K)
Ceramic	1270		9.3
Plexiglas	350	380	80
Ertalon 6 SA	350-370	~ 480	95
Vespel SP1	570		54

Table 11-2: Properties of different materials used as support for the ceramic heads

The support of the ceramic heads is illustrated in Figure 11-5 on the left, where the inside geometry is seen with the Plexiglas support and the exterior geometry is shown with the Ertalon support. On the same figure on the right, the geometry of the Inox stem, that sustains the support, is also shown.

When the choice of the geometry and the suitable materials are decided, the next step is the selection of a suitable adhesive for each kind of different surfaces in contact. In Table 11-3, their name together with the corresponding materials to glue together and their maximum temperature of use are given.

The final design of the probe is also published by Iliopoulou and Arts (2005).

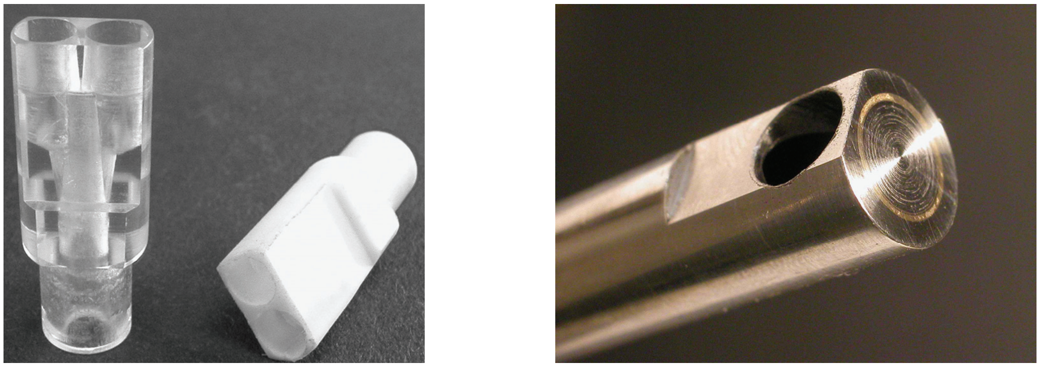

Figure 11-5: Plexiglas or Ertalon Support and Metal Stand

Name of the glue	Materials of the glued surface	Max. Temperature of use (K)
MetalTec MT7150	Vespel – Ceramic Vespel – Steel	530
Loctite Metal Set S2	Steel – Plexiglas Steel – Ertalon	390
Cyanolit	Ceramic – Plexiglas Ceramic – Ertalon	350
Celastic	Ceramic Head – Heating Element	~520

Table 11-3: Different glues used in assembling the parts of the dual thin film probe

11.3 Measurement chain and Calibrations

Each gauge has to be submitted to a resistance/temperature calibration as it acts as a resistance temperature thermometer. The resistance changes of the gauge are acquired through a Wheatstone bridge, whose voltage output needs also to be calibrated. An indication of the sensitivity of the gauges as a resistance thermometer, Eq. (1), and of the Wheatstone bridges, used for the next set of experiments, is shown in Table 11-4. The wall heat fluxes ($Q_{W1,2}$) that depend on the thermal effusivity of the substrates can be evaluated by the Fourier law at the gauge surfaces and be expressed as a function of the wall temperatures $Q_{W1,2} = f\,(T_{W1,2}\,,t)$ through Eq. (31).

Gauge	Resistance Thermometer	Wheatstone Bridge	Post processing for the determination of Q_W
Hot	$T_{W1} = 13.149\ R_1 - 430.91$	$d_{\Delta R}/d_{\Delta V} = 1.6466$	1D conduction in spherical coordinates
Cold	$T_{W2} = 13.288\ R_2 - 426.53$	$d_{\Delta R}/d_{\Delta V} = 1.4622$	1D conduction in spherical coordinates

Table 11-4: Measurement chain: Sensitivity of the gauges (Resistance-temperature calibration) and of the Wheatstone bridges for each gauge for the Plexiglas support D.T.F.P. in CT2

In Eq. (31), it is obvious that for the gas temperature calculations, only the ratio of the two wall heat fluxes is used and not their absolute value independently. Thus, only the knowledge of the ratio of the thermal products of the two gauges ($\sqrt{(\rho c k)_1} / \sqrt{(\rho c k)_2}$) is needed, for the accurate determination of the gas temperature. In paragraph 10.7, where the procedure to calibrate this ratio of the thermal products is described, it is experimentally proven that two nominally identical ceramic hemispheres have the same value of thermal product and thus their ratio is equal to *1*.

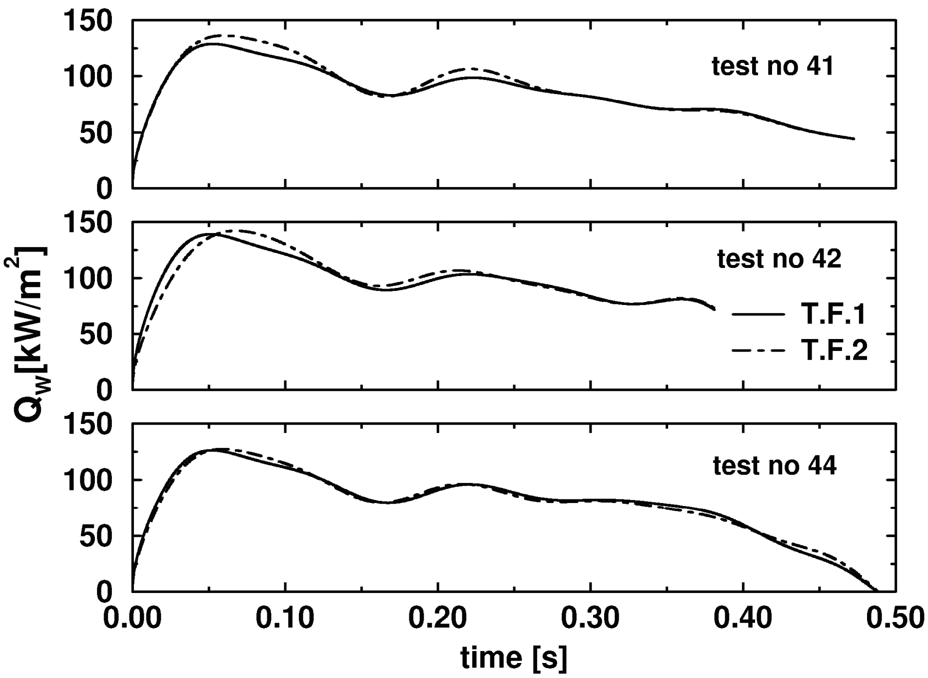

Figure 11-6: Wall heat fluxes during calibration of the Plexiglas support D.T.F.P. in CT2

However, in practice, it is always recommended to also determine the ratio of the two thermal products for every new probe that is assembled with a simple test: the two gauges are introduced in the same flow under the same initial conditions. Then the corresponding wall heat fluxes are calculated by using the same value of the thermal product for both gauges. If there are differences between the thermal product values, the wall heat fluxes are not equal. Three of such tests are performed in CT2, for the Plexiglas support probe, by keeping the initial temperature of both gauges ambient (no heating). The value of the thermal product for the heat flux calculations is $2073\ J/(m^2Ks^{0.5})$, which is the calibrated one for ceramic substrates by the electrical discharge method (paragraph 3.8). The calculated wall heat fluxes from the three above tests are shown in Figure 11-6 (each graph corresponds to a test and contains the wall heat flux from both gauges (T.F.1 and T.F.2)). The differences between the two wall heat fluxes of the same test are small and they are mainly introduced by noise problems or a small local non-uniformity of the flow. Thus, for the next series of experiments with the Plexiglas support probe, the value of the ratio of the thermal products is taken equal to one. Please note that both temperature histories are primary low pass filtered at *10Hz* (see paragraph 11.4).

11.4 Measurements in CT2 with the Plexiglas support probe

11.4.1 Dual thin film probe in fixed position between two blades

The gas temperature calculations with the dual thin film probe requires that both heads are exposed to the same flow, therefore the probe operation is suitable for two dimensional flow fields. For the tests described in this paragraph, in order to avoid the three dimensional perturbations of the blade wake, the probe is placed in between two blades behind the cascade of Figure 11-1.

During the blowdown, the wall temperature variation with time for each thin film is monitored (sampling frequency of *10KHz*) and shown in the first graph of Figure 11-7. Then the wall heat fluxes (third graph) and the gas temperature (second graph) are calculated. The two wall temperatures after *0.4s* are increased by *6K* and *22.7K* for the hot and cold gauge respectively, while the initial values are *370.2K* and *333.5K*. Note that the cold head is also heated by natural convection, radiation and conduction through the probe support. The corresponding wall heat fluxes reach values up to $19kW/m^2$ and $74kW/m^2$. The fluctuations on the gas temperature are generated by the oscillations of the piston in the tube of the CT2 facility (paragraph 1.5) during the test. More specifically, at one side of the piston, air flow is entering the tube from the high pressure reservoir and pushes the piston forward. The air at the other side of the piston in the tube is compressed till the desirable values of temperature and pressure. Then the shutter opens and the volume flow rate into the tube from the reservoir must equal to that flowing out through the test section in the dump tank. However, when the shutter opens, a difference on the air velocities is occurred between the inlet flow and the exit flow at either end of the tube. The piston can not respond instantaneously to this velocity difference due to its finite mass. As a result, it starts to oscillate and compress and decompress the flow at the test section, occurring pressure and temperature fluctuations (Jones et al., 1973).

The Wheatstone bridge output for both gauges is numerically low pass filtered at *10Hz*. On one hand, such a strong filter eliminates all the possible oscillations on the temperature signal that are generated by noise on the measured wall temperature. On the other hand, although, the piston oscillations can still be captured, as their frequency is less than *10Hz*, their shape deteriorates to less abrupt variations than in the real case. Note that in the analysis that follows the next chapters, the low pass filtering is performed at *100Hz*, however, at this point of the analysis, it is promising that the noise is completely eliminated from the low frequency component of the gas temperature by filtering it at *10Hz*, in order to study in detail every parameter that influences the gas temperature calculation.

Another look at Eq. (45) shows that the values of the two wall heat fluxes should be sufficiently different, so that their ratio is ‘far’ from *1* and the gas temperature calculation is possible. The first attempt to provide more quantitative information on the above concept is to bring one of the two initial wall temperatures close to the gas temperature, so that the corresponding wall heat flux tends to zero during the test (Iliopoulou and Arts, 2002). In paragraph 10.6, it is numerically demonstrated that by only changing the wall heat flux ratio from *0.737* to *0.079* keeping the same sampling frequency and the same noise on the wall temperature signals, the noise on the gas temperature reduces four times. For the test presented in Figure 11-7, the initial wall temperature of the hot gauge is chosen close to the expected gas temperature.

Any kind of higher difference between the two wall heat fluxes is sufficient to calculate a low noise gas temperature signal. The above difference can be higher, either by forcing the wall heat flux of the cold gauge even closer to zero, or just by increasing the initial wall temperature difference between the two gauges. In Figure 11-8, this difference is shown as a function of initial temperature of the hot gauge. The interesting part of this figure is that the higher the heating is for the hot probe, the higher the initial temperature difference becomes. However, care should be taken not to exceed the maximum operating temperature of the different materials of the probe.

Another way to reduce the noise on the gas temperature calculations is to reduce the sampling frequency. In paragraph 10.6, it is shown that the noise levels on the calculated wall heat flux depends on the sampling frequency. The higher the sampling frequency is, the higher the noise is on the heat flux and inevitably on the gas temperature calculations.

The results from the gas temperature calculations are compared with the measurements from a $90\mu m$ wire type K thermocouple placed upstream of the cascade. The sensitivity of the combination Chromel - Alumel is $40\mu V/K$ and the signal is amplified by a factor of almost *1000*. Using a recovery coefficient equal to *0.68* the velocity error is also minimized (Arts and Charbonnier, 1994). Because there is no rotation of the blades, thus no extraction of work, the total gas temperature remains constant, as the flow passes through the cascade at a streamline far from the blade walls, where the flow can be considered adiabatic. (Note that close to the blade walls, energy is transmitted from the hot flow to the cold blades creating the total temperature wake behind the blade.) Four test results, where the dual thin film probe is placed between two blades (hence no influence of the wake of the blade on the gas temperature calculations), are shown in Figure 11-9.

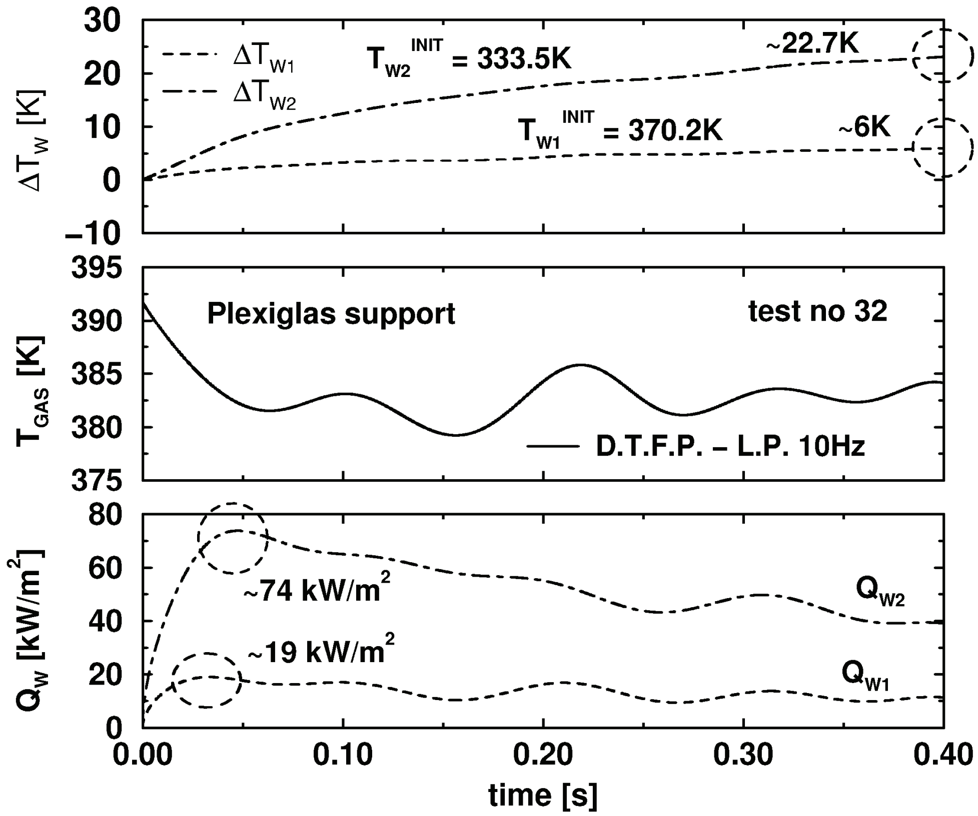

Figure 11-7: Wall temperatures, gas temperature calculations and corresponding wall heat fluxes (Plexiglas support D.T.F.P. in CT2 between two blades)

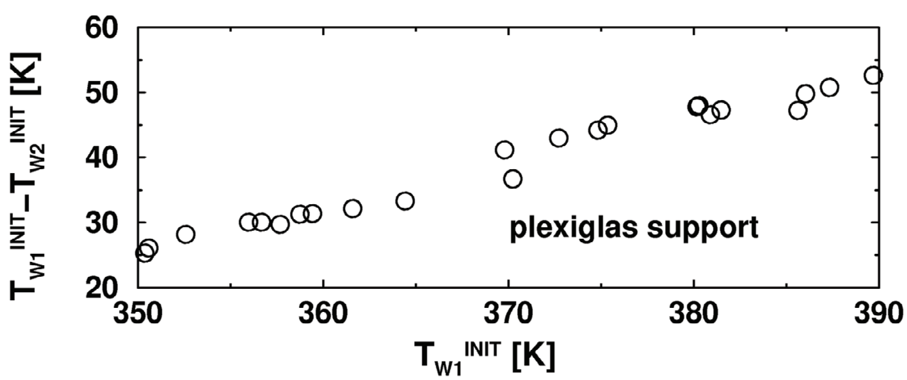

Figure 11-8: Initial wall temperature difference between the two gauges (Plexiglas support D.T.F.P. in CT2)

The average gas temperature value calculated from the dual thin film probe results looks to be quite close to the values obtained by the thermocouple. The oscillations of the gas temperature are mainly due to the oscillations of the piston inside the tube of the facility, during the test time. However, it is obvious that the probe responds much faster than the thermocouple.

Therefore, the unsteady compensation of the thermocouple is of primary importance for comparing the signals of the two different probes.

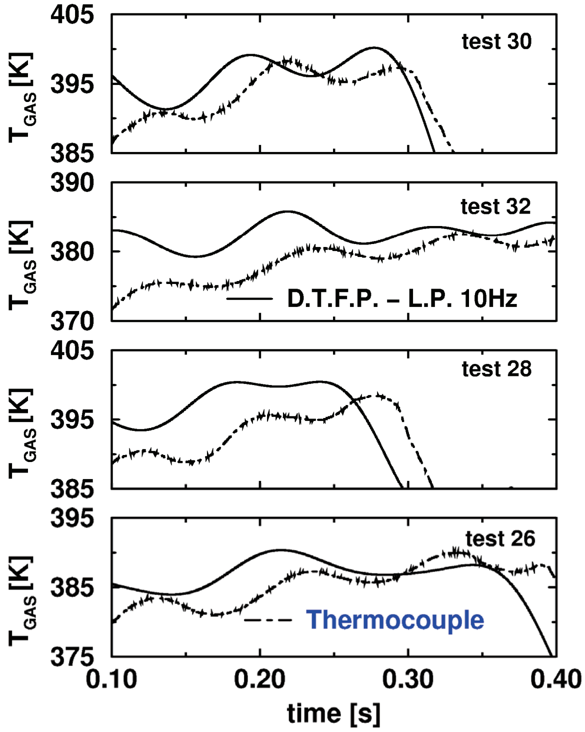

Figure 11-9: Comparison between the D.T.F.P. and the thermocouple (Plexiglas support D.T.F.P. between two blades)

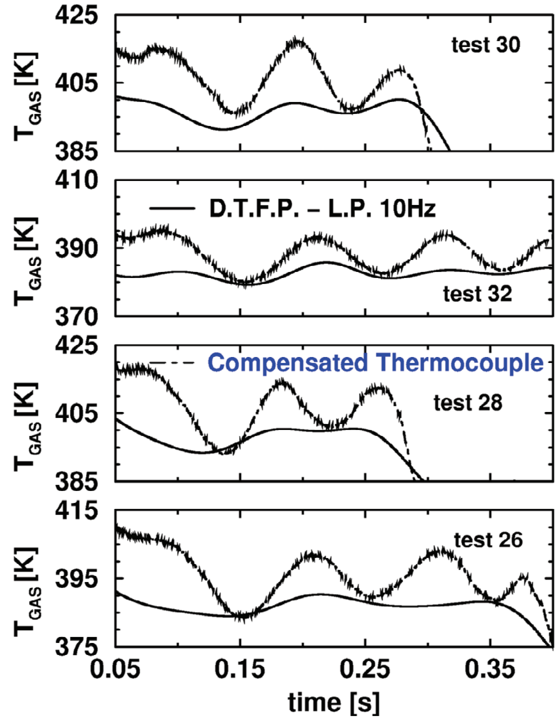

Figure 11-10: Comparison between the D.T.F.P. and the compensated thermocouple (similar to Figure 11-9)

The response of any thermocouple can be simulated with a combination of two discrete first order systems. Wires and junction are considered independently as first order systems, which correspond to a thermocouple with different junction and wire diameters. The conduction to the support is considered negligible. A direct least-squares algorithm is implemented for the determination of the parameters of the above linear systems (Paniagua et al., 2002). The dynamic calibration of the thermocouple used in the CT2 facility is performed by a second similar one, with the same diameter and length of the wires, in a jet coming out from a *22mm* diameter nozzle. The thermocouple used in the CT2 facility just broke after the last test. The second thermocouple is located perpendicularly to the flow, *20mm* downstream of the nozzle, and a plate between them deflects the flow. Then the plate is rapidly opened and the second thermocouple is exposed to a sudden change of temperature. The smallest time constant was found *68ms* for a Reynolds number of the order of *270* depending on the wires diameter of the thermocouple, which is not so far from the equivalent value given by Paniagua et al. (2002) for the same type of thermocouples It is *45ms* in their case but for wires parallel to the flow.

The comparison between the dual thin film probe and the compensated signal of the thermocouple used in the CT2 facility is shown in Figure 11-10. The compensated average value of the thermocouple signal is considerably increased around *10K* and the amplitude of the temperature oscillations is also significantly amplified as a result of the compensation. Both changes seem to be exaggerated. It is possible that the dynamic calibration of the thermocouple used in the CT2 facility is slightly different than the one of the second thermocouple. In addition, the Reynolds number for the tests in the CT2 facility is estimated *400*, higher than the one used for the dynamic calibration (*270*). The difference in Reynolds number is mainly due to the higher velocity in the CT2 facility, something that eventually leads to higher heat transfer rates and so, higher response from the thermocouple junction. Thus, the compensation of the thermocouple based in a lower Reynolds number is over estimated. This is a second reason that can explain the high temperature oscillations on the compensated signal (Figure 11-10). Last but not least, big part of the stem of the thermocouple is exposed to the flow during the CT2 tests, contrary to the dynamic calibration tests, where only a very small part of the stem feels the hot flow. That's an additional reason to believe that the compensation of the thermocouple is overestimated.

In general, the compensation of the thermocouple is a numerical tool to reconstruct part of the lost signal but it has to be used with precaution. In our case, the thermocouple compensation is not used for the average total temperature values, but mainly for the determination of the period of the fluctuations on the gas temperature due to the piston oscillations. The minimum-maximum of the temperature fluctuations appear at the same time when determined by the compensated thermocouple and by the probe.

The gas temperature is also calculated by low passing the wall temperature signals of the two gauges at *30Hz* (Figure 11-11), in order to investigate the influence of filtering. Not only the amplitude of the oscillations is increased, but also oscillations that follow a higher frequency appear. In addition, a temperature peak appears at the beginning of most of the tests.

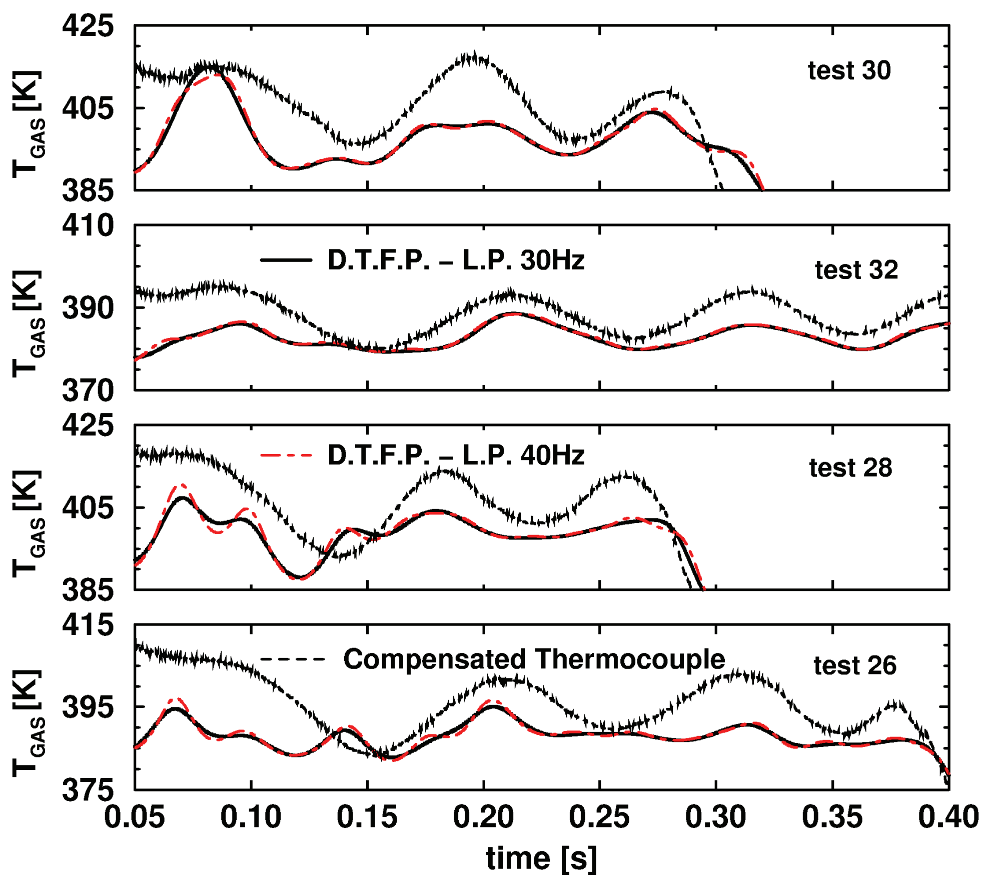

Figure 11-11: Total temperature low pass filtered at 30 and 40Hz (D.T.F.P. between two blades)

Note that the numerical filter used in the present analysis is a fifth order Butterworth filter whose analog and digital design is provided by the numerical tool 'Matlab'. The Butterworth filter is not as sharp cut-off filter as the Chebyshev and the elliptic filters, although it is sharper than the Bessel-Thomson filter or the Hanning window. The latter two function filters better approximate the Gaussian function (contrary to Butterworth filter that shows overshooting and ringing) but they are not supported by 'Matlab' digital data filtering. Thus, the selected

Butterworth filter could be responsible for the above higher frequency oscillations observed on the gas temperature, when the filter frequency of the wall temperatures increases (Iliopoulou and Arts, 2005).

The signals of the two gauges are also filtered at *40Hz* and the corresponding gas temperature is compared with the previous signals in Figure 11-11. Although there are no additional oscillations, it appears that the maximum of the existing ones has increased for some of the measurements. In addition, when a Fast Fourier Transformation (FFT) is applied on the filtered and unfiltered temperature signal of the cold gauge (by first subtracting the mean value of the signal for better resolution) (Figure 11-12), the *10Hz* low pass filter deteriorates the signal significantly. Thus, by filtering at *10Hz*, information is lost on the wall temperature signals and as a consequence on the gas temperature calculation. The measurements should be repeated in such a way that even higher values of the low pass filter on the wall temperatures could lead to a trustful gas temperature determination (see chapter 12). Further increasing of the low pass filter limit on the wall temperatures of this series of tests introduces very high noise on the gas temperature calculations.

The additional oscillations generated by increasing the low pass filter limit could more possibly be a result of unsteadiness or local non-uniformity of the flow. However, the frequency of the oscillations is low and their amplitude high; this could point the answer more towards non-uniformity from a physical point of view.

The noise associated to the thin film temperature signals highly increases on the wall heat flux calculations according to the sampling frequency (*10 kHz* for this case) and then increases even more for the gas temperature calculations, based on the ratio of the two heat fluxes. Numerical simulations (paragraph 10.6) have shown that a noise of *0.005 K* on the wall temperature signals introduces about *65K* noise on the gas temperature with a sampling frequency of *10 kHz* and a heat flux average ratio of *0.7*. Thus, for the second series of tests (chapter 12), the sampling frequency was decreased to *1kHz*.

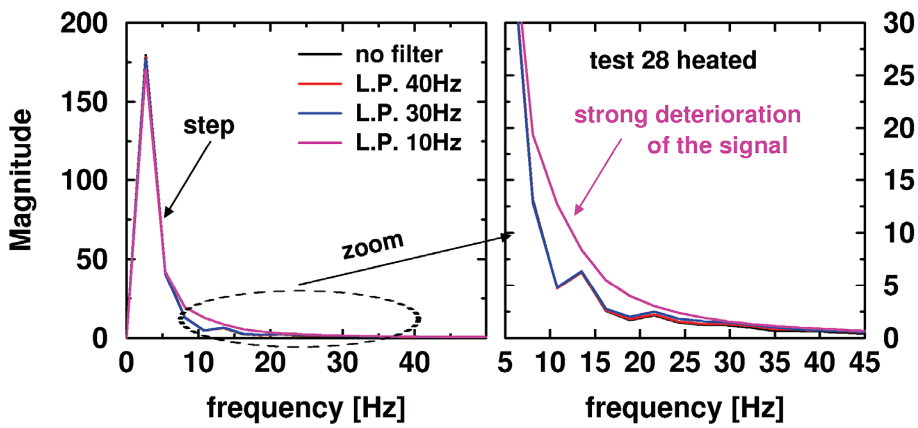

Figure 11-12: FFT on the wall temperature of the cold gauge of the Vespel support D.T.F.P.

11.4.2 Dual thin film probe in traverses downstream a cascade

Measurements are also taken by traversing the dual thin film probe behind the cascade in CT2. The total traversing distance is 1.24 blade pitches, so one blade wake is clearly seen at the recording time around *0.16s* in Figure 11-13. The wall temperature signals are low pass filtered at *10Hz* and the thermocouple is at the same stable position as previously, upstream of the cascade. In Figure 11-14, the wall temperatures are low pass filtered at *30Hz* and the thermocouple is compensated. It seems that when the probe is out of the blade wake (last half part of the signal – recording time from *0.23* to *0.28s*), a delay is observed in the total gas temperature fluctuations that are generated by the piston movement. The last observation is in contrast with the measurements taken for a fixed position of the probe, described in 11.4.1, where the gas temperature oscillations measured by the probe and the compensated thermocouple seem to be in phase.

In Figure 11-15, a Fast Fourier Transformation (FFT) is applied on the raw voltage signals of the gauges after being high pass filtered at *2Hz* to eliminate the mean values. Both wall temperature signals and both experiments (a traverse and a stable position of the probe between two blades) are examined. The major peak generated on both signals for the stable position test is around *14 Hz* and is due to the piston oscillations. On the contrary, the major peak on the traversing signals is observed earlier at *10 Hz* for the hot thin film and *12Hz* for the cold thin film. Please, notice that the two peaks do not have the same frequency: these differences are probably the result from a combination of phenomena in the traversing case that interact with each other. A phenomenon that follows such low frequencies can be mainly mechanical. While the probe traverses, the resonance for each head of the probe can be different, as the former depends on the stiffness and the assembly procedure of each head. Note that the ceramic heads are the same in terms of geometry and material, however, inside one of them, there is in addition the heating element (Figure 11-4). Thus, the resonance of each head can be the reason for the delay of the piston oscillations on the gas temperature calculations with the probe.

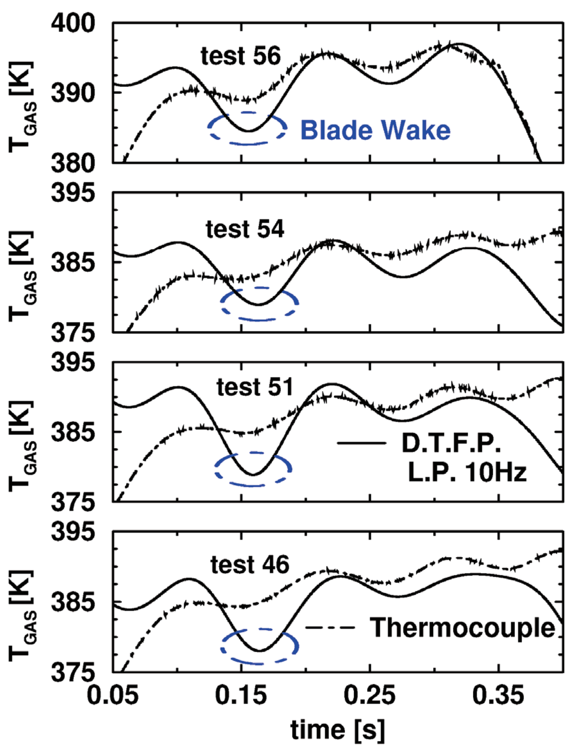

Figure 11-13: Total temperature low pass filtered at 10Hz and thermocouple (Plexiglas support D.T.F.P. at traverses)

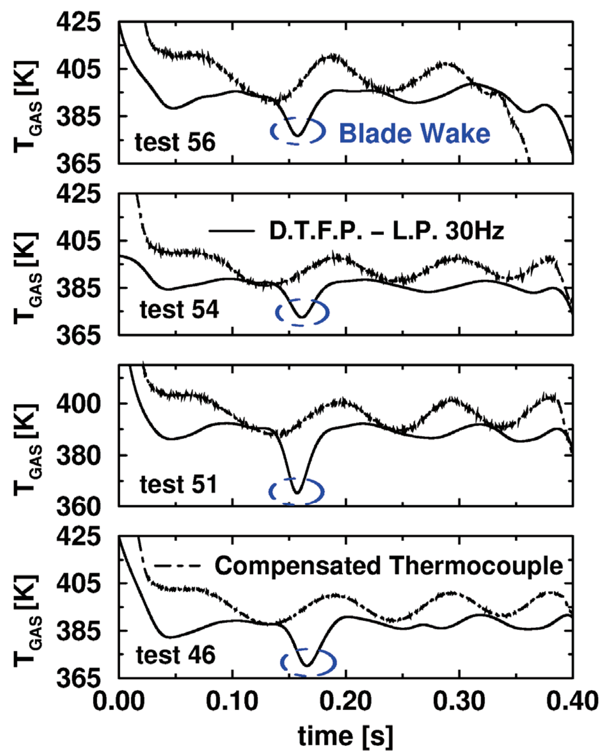

Figure 11-14: Total temperature low pass filtered at 30Hz and compensated thermocouple (Plexiglas support D.T.F.P. at traverses)

The distance of the traversing mechanism from its starting position (*ΔL=0* for *t=0*) with respect to the experimental time is also measured, and the position of the blade is shown in Figure 11-16 (indicated with the blue dashed line). The blade wake can be identified by the probe in terms of total temperature deficit. Because of the high three dimensionality of the flow and the small spatial resolution of the probe (the distance between the two thin films is *4.2mm*, see Figure 11-3), the two heads do not see exactly the same flow. As a result, the gas temperature calculations when the probe is just behind the wake suffer from accuracy; the calculated value is highly influenced from the filtering: by low pass filtering in higher frequency, the amplitude of the gas temperature deficit increases. However, when the probe is used to determine rotor blade wakes (paragraphs 14.3 and 14.4), the high frequency periodicity of the flow enables the functionality of the probe to measure average values (e.g. The rotor blade passing frequency in the CT3 facility is *6.9KHz*, while the two wall temperatures are low pass filtered at *100Hz*, thus the calculated gas temperature is an average of *69* wakes.) (time-averaged measurements, paragraphs 14.3.1 and 14.4.1). In addition the average gas temperature fluctuations due to the blade wakes can also be determined when a phase locked average is performed on the recorded wall temperature signals (time-resolved measurements, paragraphs 14.3.2 and 14.4.2).

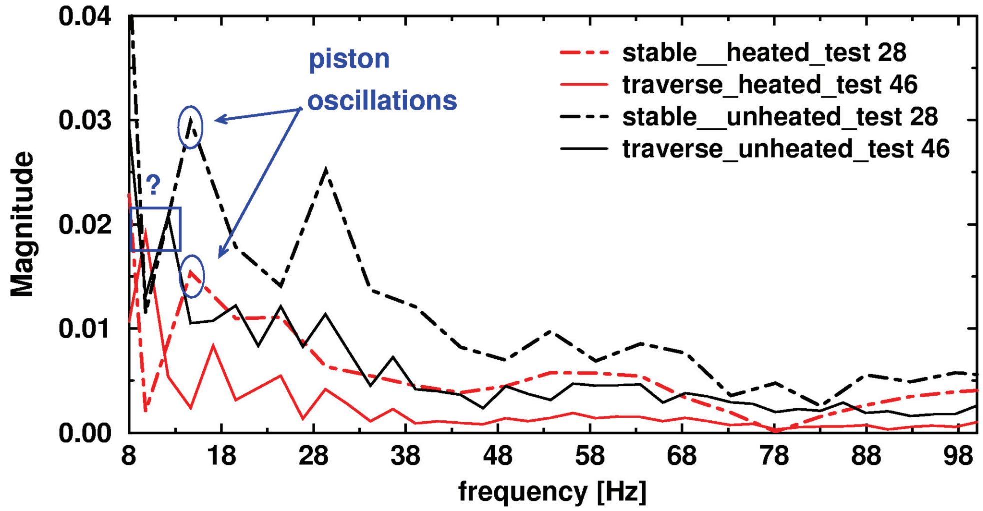

Figure 11-15: FFT on the raw W/B voltage signals of the gauges after being high pass filtered at 2Hz to eliminate the mean values (Plexiglas support D.T.F.P. in CT2)

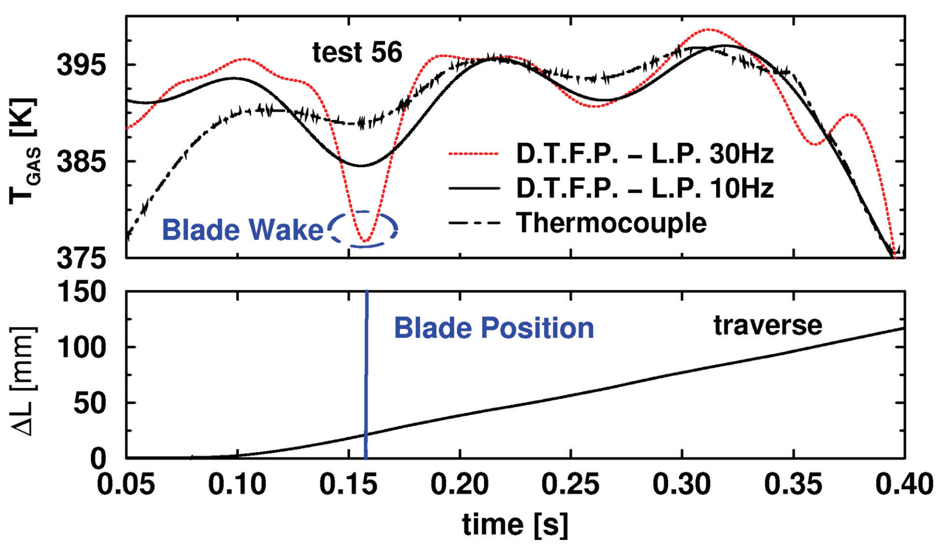

Figure 11-16: Position of the blade and the generated wake on the gas temperature (Plexiglas support D.T.F.P. in CT2)

According to Figure 11-16, the speed of the traverse is *120mm* in *0.3s* that corresponds to *0.4m/s*. The outlet Mach number of the flow is *1.07* corresponding to a velocity of *395m/s*. Even after every shock wave upstream the two heads of the probe, the flow velocity is still two orders of magnitude higher than the traversing velocity. Thus, no apparent influence of the traverse would be expected on the flow direction that the heads feel. Therefore, no significant movement of the stagnation point should be considered. In addition, although the shock waves upstream of the probe could interfere with the wakes and shock waves of the blades, once the probe feels the streamlines far from the blade walls, no additional influence is expected. The two last conclusions enforce the concept that the delay of the oscillations on the gas temperature calculations during the traverse of the probe is due to the resonance of the two heads.

The position of the blade wake is easily recognized on the probe wall temperatures and heat fluxes in Figure 11-17. The two temperature signals were low pass filtered at *30Hz* and the calculated gas temperature is compared with the compensated value given by the thermocouple.

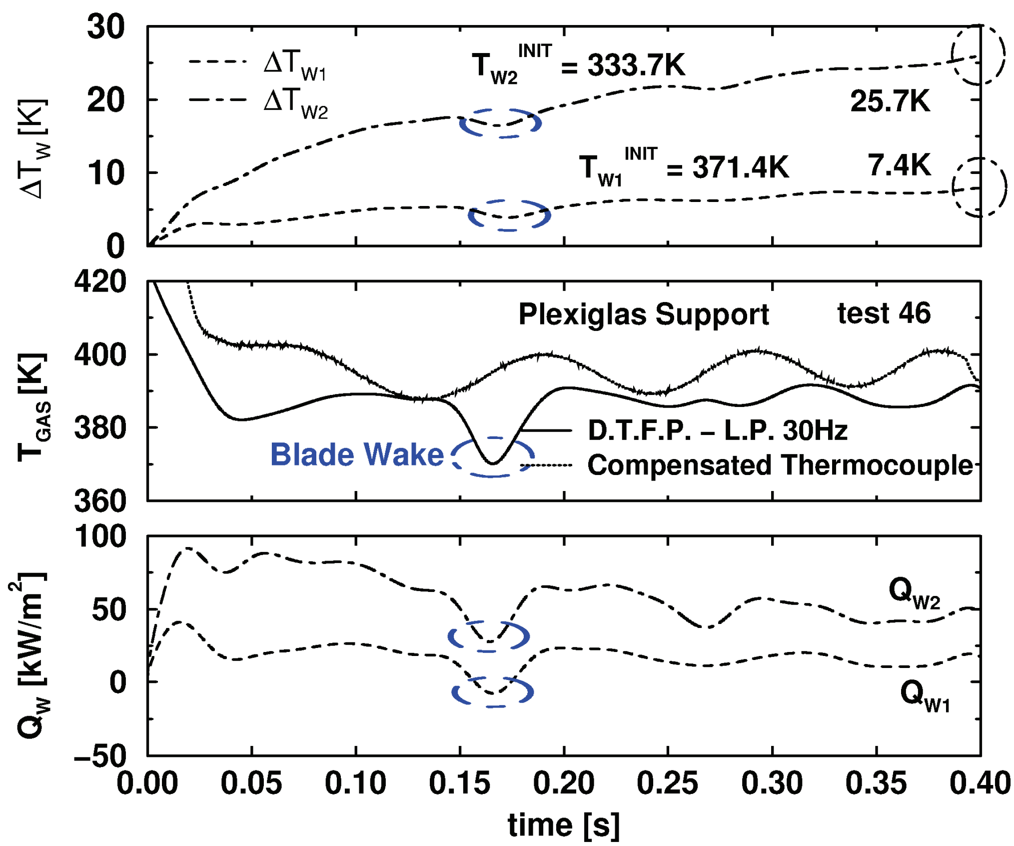

Figure 11-17: Wall temperatures, gas temperature calculations and corresponding wall heat fluxes (Plexiglas support D.T.F.P. at traverses)

11.4.3 Conclusions and repeatability

An attempt to quantify the above results is shown in Table 11-5. The average value of the gas temperature is given twice, once calculated from the dual thin film probe results and once measured by the thermocouple. The wall temperature signals are low pass filtered at *10Hz* and the thermocouple signal is not compensated. Both average values are taken for a period of gas temperature oscillations, close to the end of the test, so that the thermocouple reaches the real gas temperature and the probe is always far from the blade wake for the case of the traversing measurements.

The upper left part of Table 11-5 consists of measurements with an initial temperature difference between the two gauges of the probe less than *30 K*. Note that the temperature of the heated gauge for the above cases is more than *30-35 K* lower than the actual value of the gas temperature. Such kind of initial conditions lead to high noise on the gas temperature calculations. On the contrary, the more the initial temperature of one gauge approaches the actual gas temperature, the less the signal is influenced by noise and the better is the accuracy on the gas temperature calculation. The reason for the above observation is based on Eq. (45). The more the two wall heat fluxes of the two gauges differ, the smaller is their ratio. In addition, according to Figure 11-8, the higher the heating is, the higher the difference of the initial wall temperatures of the two gauges becomes, and the corresponding wall heat flux ratio decreases. Thus, for every gas temperature value, there is a minimum difference on the initial wall temperatures that results in an acceptable level of noise on the gas temperature. This minimum difference is only reached from test 24 in Table 11-5. The measurement uncertainty of the tests from 24 to 57 is ± *4K*.

Test	$T_{D.T.F.P.}$ (K)	T_{THERMO} (K)	$T_{D.T.F.P.} - T_{THERMO}$ (K)	Test	$T_{D.T.F.P.}$ (K)	T_{THERMO} (K)	$T_{D.T.F.P.} - T_{THERMO}$ (K)
12	398.2	388.4	9.8	47	388.5	391.4	- 2.9
14	395.2	386.3	8.9	48	397.1	399.6	- 2.5
18	384.4	388.8	- 4.4	49	400.9	400.8	0.1
20	378.7	389.5	- 10.8	50	387.6	386.9	0.7
22	380.8	386.2	- 5.4	51	388.8	389.4	- 0.6
24	401.0	398.2	2.8	52	393.5	393.7	- 0.2
26	387.9	387.3	0.6	54	385.2	387.1	- 1.9
28	400.0	396.2	3.8	55	390.4	392.9	- 2.5
30	397.7	396.5	1.2	56	393.7	394.7	- 1.0
32	382.7	380.3	2.4	57	402.1	398.6	3.5
46	387.3	389.2	- 1.9				
				Average	*392.8*	*392.7*	*0.1*
				rms	*12.3*	*11.1*	*4.3*

Table 11-5: Uncertainty on the gas temperature calculated by the D.T.F.P.

11.4.4 Limitations of the basic design

It is important to mention that although the above series of experiments were successfully performed with initial conditions of the hot gauge very close to the actual gas temperature, the Plexiglas support and the Cyanolit glue that were used for this probe cannot withstand temperatures higher than *350 K*. Thus, due to the high conduction from the ceramic head to the Plexiglas support, the part of the Plexiglas that supports the hot ceramic head cracked and the glue burnt out (Figure 11-18). However, the hot head remained in place, because it was kept from the other side of the Plexiglas support, where apparently the temperature was less high as it borders with the cold head. (The possible temperature non-uniformities inside the support, due to the difference between the hot and the cold head, do not influence the wall heat flux calculations that take place at a radius of *1.5mm* from the heads stagnation point, while the support is *10mm* further.) The measurements continued till the end of the campaign. No problem is observed on the connections and the wires. For the second series of experiments (chapter 12), Vespel is selected as material for the new support; it can withstand temperatures as high as *570K* (Table 11-2) and MetalTec MT7150 is the glue that connects the Vespel support with the ceramic heads and the steel stem (Table 11-3).

In the previous analysis, the two wall temperature signals were strongly low pass filtered, at maximum *30-40Hz*. A severe consequence is the distortion of the gas temperature signal mainly at the beginning of the test. The test can be approximated by a step in gas temperature, once the shutter opens. A severe filtering on the signal can smooth this beginning of the test, in such a way that important information is lost. However, the high sampling frequency of the test introduces high noise on the gas temperature and thus requires a severe filtering. Therefore, the selection of the sampling frequency of the second series of tests in CT2 is one order of magnitude less than the above-described tests, equal to *1kHz* (chapter 12). Then the noise on the calculated gas temperature reduces and thus a low pass filtering of *100Hz* on the wall temperatures is feasible.

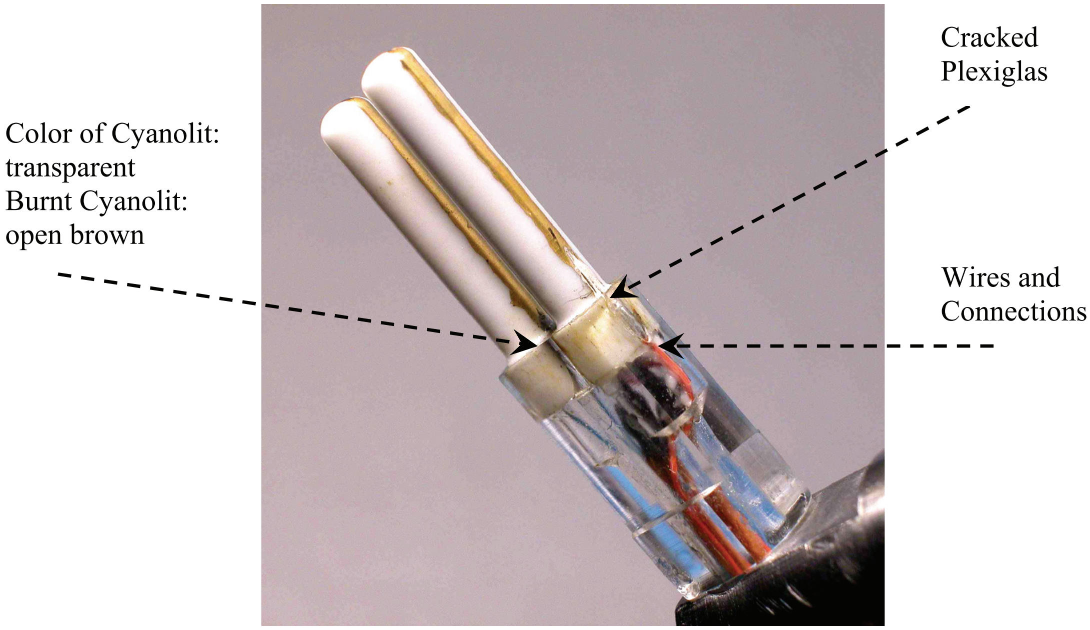

Figure 11-18: Result of overheating the Plexiglas support during the measurements in CT2

11.5 References

Arts T., Charbonnier J-M., 1994, *'Temperature measurements'*, Measurement Techniques in Fluid Dynamics, VKI LS 1994-01, ISBN D/1994/0238/417

Consigny H., Chan C.K., Richards B.E., 1979, *'The effect of pressure gradient and external turbulence on heat transfer to a cold flat plate'*, VKI TN 128

Iliopoulou V., Arts T., 2002, *'Applications of the heat flux thin film sensor in short duration flows'*, Proceedings of ESDA 2002, Istanbul, Turkey

Iliopoulou V., Arts T., 2005, '*The dual thin-film probe for high frequency flow temperature measurements'*, Proc. 6th conf. on Turbomachinery, Fluid Dynamics and Thermodynamics, Lille, France – to be published in Proc. of the Institution of Mech. Eng. Part A 'J. of Power and Energy'

Jones T.V., Schultz D.L., Hendley A.D., 1973, *'On the flow in an isentropic light piston tunnel'*, Reports and Memoranda no 3731, Dept. Engineering and Science, University of Oxford, Great Britain

Paniagua G., Denos R., Oropesa M., 2002, *'Thermocouple probes for accurate temperature measurements in short duration facilities'*, Proceedings of ASME TURBO EXPO 2002, Amsterdam, The Netherlands

Sieverding, C. H., and Arts, T., 1992, *'The VKI compression tube Annular Cascade Facility CT3'*, ASME paper 92-GT-336, Koln, Germany